DaCapo: Automatic Bootstrapping Management for Efficient Fully Homomorphic Encryption

Seonyoung Cheon *Yonsei University*
Yongwoo Lee *Yonsei University*
Dongkwan Kim *Yonsei University*
Ju Min Lee *Yonsei University*
Sunchul Jung *CryptoLab. Inc*
Taekyung Kim *CryptoLab. Inc*
Dongyoon Lee *Stony Brook University*
Hanjun Kim *Yonsei University*

Abstract

By supporting computation on encrypted data, fully homomorphic encryption (FHE) offers the potential for privacy-preserving computation offloading. However, its applicability is constrained to small programs because each FHE multiplication increases the scale of a ciphertext with a limited scale capacity. By resetting the accumulated scale, bootstrapping enables a longer FHE multiplication chain. Nonetheless, manual bootstrapping placement poses a significant programming burden to avoid scale overflow from insufficient bootstrapping or the substantial computational overhead of unnecessary bootstrapping. Additionally, the bootstrapping placement affects costs of FHE operations due to changes in scale management, further complicating the overall management process.

This work proposes DACAPO, the first automatic bootstrapping management compiler. Aiming to reduce bootstrapping counts, DACAPO analyzes live-out ciphertexts at each program point and identifies candidate points for inserting bootstrapping operations. DACAPO estimates the FHE operation latencies under different scale management scenarios for each bootstrapping placement plan at each candidate point, and decides the bootstrapping placement plan with minimal latency. This work evaluates DACAPO with deep learning models that existing FHE compilers cannot compile due to a lack of bootstrapping support. The evaluation achieves 1.21×speedup on average compared to manually implemented FHE programs.

1 Introduction

Fully homomorphic encryption [22] (FHE) has emerged as a promising solution for privacy-preserving computation in untrusted environments, like financial and healthcare applications on a third-party cloud. FHE allows computations on encrypted data, and its decrypted results are identical to those obtained from unencrypted computations. Since Gentry's pioneering work on FHE using lattice-based cryptography [22], many FHE schemes [8,11,12,14,20], and supporting libraries [1, 2, 17, 21, 25, 26, 46, 48, 54] have been proposed. Among the FHE schemes, RNS-CKKS [11] is suitable for privacy-preserving machine learning models as it offers optimized fixed-point arithmetic and SIMD support.

In RNS-CKKS, a ciphertext embeds a scaled integer with the maximum scale capacity, called *coefficient modulus Q*. Each FHE multiplication increases its accumulated scale, like the multiplication of two scaled numbers. When the accumulated scale exceeds the coefficient modulus Q, scale overflow occurs, leading to an unrecoverable result. Thus, programmers should carefully design an RNS-CKKS program with a limited number of multiplications, or insert *bootstrapping* [10] operations that reset the accumulated scale of a ciphertext, enabling a longer multiplication chain. Although existing RNS-CKKS compilers [18, 39, 41] can automatically manage ciphertext scales reflecting constraints of RNS-CKKS operations, their applicability remains limited to small RNS-CKKS programs due to lack of bootstrapping support. Only manual bootstrapping placement [36, 38] has been proposed for a long FHE program such as ResNet, but the manual placement imposes a significant burden on programmers and easily leads to inefficient performance.

Optimizing a long FHE program with manual bootstrapping placement is challenging for three reasons. First, programmers should trace the growth of the accumulated scale of each ciphertext, and insert the bootstrapping operation before scale overflow occurs. Second, a bootstrapping operation has significant latency, which is the most expensive among RNS-CKKS operations. While avoiding scale overflow from insufficient bootstrapping, programmers should reduce the number of bootstrapping operations, not to unnecessarily increase bootstrapping overheads. Third, bootstrapping placement affects scale management. Since bootstrapping resets the accumulated scales of ciphertexts, and RNS-CKKS operations have different latencies depending on their accumulated scale, the bootstrapping insertion points change the latencies of the other RNS-CKKS operations. Therefore, to optimize bootstrapping placement, the number of bootstrapping operations and their performance impact on the other RNS-CKKS operations should be considered together.

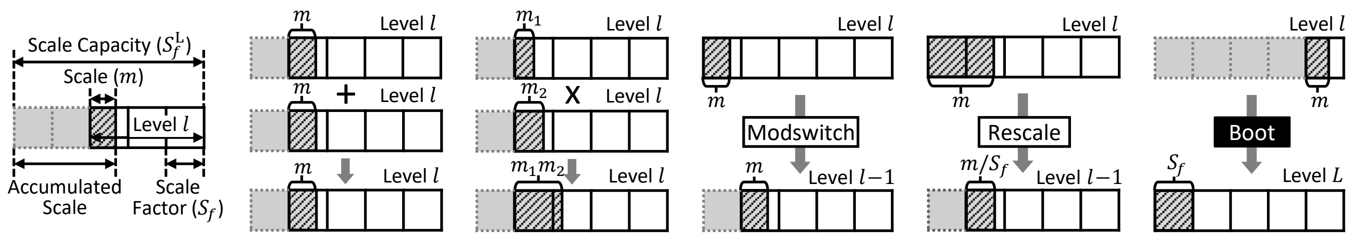

(a) Definition (b) Addition (c) Multiplication (d) Modswitch (e) Rescale (f) Bootstrapping

Figure 1: RNS-CKKS operations. Additions and multiplications require the input operands to have the same level l. Additions additionally require the operands to have the same scale m. The `modswitch` and `rescale` operations reduce level l by one; the `bootstrap` operation resets the level l to the initial level $L = 5$.

This work proposes DaCapo, the first automatic bootstrapping placement compiler that heuristically places bootstrapping operations to minimize the overall latency in an FHE program. To reduce the number of bootstrapping operations, DaCapo analyzes live-out ciphertexts, which are used by later instruction at each program point, and classifies program points with a minimal number of live-outs as a candidate set of bootstrapping insertion points. DaCapo identifies a subset of the live-out ciphertexts that remain unused for a certain period without requiring bootstrapping, and categorizes them as bypass edges. DaCapo excludes the bypass edges from the live-outs and thus achieves more precise required bootstrapping counts. To reflect the latency of the other RNS-CKKS operations, such as multiplications and rotations, affected by scale management and bootstrapping insertion points, DaCapo estimates their latency under different scale management scenarios for each bootstrapping point and finds a bootstrapping placement plan with minimal latency among the candidate set.

This work implements DaCapo compiler on top of MLIR [33] with a GPU-accelerated RNS-CKKS library called HEaaN [25]. This work evaluates DaCapo with six deep learning models such as ResNet20, ResNet-44, AlexNet, VGG-16, SqueezeNet, and MobileNet. This work implements the deep learning models with maxpooling and ReLU like the original models and also implements the same models with average pooling and SiLU that require a shorter multiplication chain. The evaluation results show that DaCapo achieves 1.21×speedup on average for diverse deep learning models, compared to the manually implemented FHE programs.

Followings are the contributions of this work.

- The first automatic bootstrapping management compiler, DaCapo, for fully homomorphic encryption;
- A new liveness-aware bootstrapping placement analysis that generates an insertion point candidate set with minimal live-out counts;
- A new cost-aware bootstrapping placement that reflects different FHE computation costs under different scale management affected by bootstrapping placement plan.

2 Background

This section describes RNS-CKKS [11] and scale management for RNS-CKKS programs. In contrast to other FHE schemes [8,12,14,20,22], RNS-CKKS provides better support for fixed-point arithmetic and SIMD parallelism by leveraging approximation (*i.e.,* encrypted computation results could be slightly different from unencrypted ones). These properties make RNS-CKKS well-suited for machine learning applications that can accommodate a certain level of approximation.

2.1 RNS-CKKS Encoding and Encryption

RNS-CKKS introduces two encoding and encryption parameters: *polynomial modulus degree* N and *coefficient modulus* Q. RNS-CKKS encodes a vector containing real numbers into a cyclotomic polynomial [7] whose degree is N. N affects the security level (*e.g.,* equivalent to 128-bit security) and the latency of RNS-CKKS operations. Q determines the maximum coefficients of the polynomials. RNS-CKKS encrypts the plaintext μ into a ciphertext, which is a pair of polynomials $(-a \cdot s + \mu + e, a)$ with random noises (a and e) and the secret key (s). The security of RNS-CKKS relies on the hardness of Ring Learning with Errors (RLWE) [42].

An RNS-CKKS ciphertext has a *scale* and a *level* property, defined as follows. RNS-CKKS deals with a polynomial with integer coefficients and encodes a real number as an integer over a *scale*. For example, the number $x = 1.1$ is encoded as an integer $v = 11$ with the scale $m = 10^1$. The multiplication of two scaled numbers increases the result's scale: *i.e.,* the scale of a ciphertext gradually accumulates on a multiplication. For instance, $y = x \cdot x$ leads to an integer $v = 121$ with the scale $m = 10^1 \cdot 10^1 = 10^2$. The scale is limited by the maximum scale capacity (defined by *coefficient modulus* Q), which is described as a product of the small fixed-size scaling factors S_f: *i.e.,* $Q \approx {S_f}^L$, where L is the initial level. The *level* l denotes the number of scaling factors S_f available in the ciphertext.

Figure 1a illustrates an RNS-CKKS ciphertext with scale and level. The ciphertext has the maximum scale capacity ${S_f}^L$

Table 1: FHE Parameters and their descriptions. The rightmost column represents the values used in actual evaluation.

Parameter	Description	In our evaluation
N	Polynomial modulus degree	2^{17}
Q	Coefficient modulus	2^{1479}
S_f	Rescaling factor	2^{51}
L_{max}	Maximum level of ciphertext	29
L	Level after bootstrapping	16

where the initial level $L = 5$ (depicted with five boxes). Starting from the initial level L, the level l decreases on `modswitch` and `rescale` operations and becomes reset to the initial level L on `bootstrap` operation (which will be explained later). Two dotted gray boxes on the left represent two scale factors consumed by `modswitch` or `rescale` operations, rendering the current level $l = 3$. The *accumulated scale* denotes the total scale accumulated (by multiplications) so far, and it should be lower than the scale capacity ${S_f}^L$. Otherwise, the scale overflow occurs, leading to an irrecoverable result. The *scale* m excludes the consumed scale factors and it should be larger than the predefined minimum scale, called *waterline* S_w, to control the noises introduced by RNS-CKKS operations.

Table 1 shows description and values of FHE parameters used in the evaluation, including a polynomial modulus degree (N) of 2^{17}, and a ciphertext can contain 65536 elements. The evaluation uses a coefficient modulus composed of primes with the same scaling factor (R) of 51 bits, and its value is equal to 2^{1479}. The bootstrapping implementation provided by library consumes 13 levels. In other words, when bootstrapping is performed using parameters with a maximum level of L_{max}, the resulting ciphertext will have 16 levels (L).

2.2 RNS-CKKS Operations

2.2.1 Arithmetic and Rotation Operations

RNS-CKKS supports basic arithmetic and rotation operations, which can be used to implement application algorithms.

Addition (Figure 1b) and **Multiplication** (Figure 1c): RNS-CKKS supports two vectorized arithmetic operations: addition and multiplication. These operations add/multiply two ciphertexts (`CAdd` and `CMul`, respectively) or one plaintext and one ciphertext (`PAdd` and `PMul`). The addition operation requires the levels and scales of two operands to be the same, and produces a ciphertext of the same level l and scale m. On the other hand, multiplication requires only the levels of two operands to be the same. The scale of the resulting ciphertext accumulates to the product of the scales of the operands: *i.e.,* $m = m_1 \cdot m_2$. Table 2 presents the runtime latency of (some) RNS-CKKS operations at different levels measured in the GPU-accelerated HEaaN library [25]. Multiplications are slower than additions. Arithmetic operations at a high level are more expensive than ones at a low level.

Table 2: Latency of FHE operations for different levels (μs)

Operation	Level						
	4	6	8	10	12	14	16
PAdd	24	32	40	47	54	64	70
CAdd	33	44	54	65	74	85	94
PMult	214	304	385	459	533	604	675
CMult	1218	1513	1795	2306	2572	2927	3151
Rot	890	1080	1239	1699	1864	2035	2225
Boot	354762						

Rotation: For vectorized arithmetic operations, RNS-CKKS additionally supports the `rotate` operation that performs a circular shift on a message vector by a given offset: *e.g.,* rotating $(a_1, a_2, ..., a_{10})$ by offset 2 leads to $(a_3, a_4, ..., a_{10}, a_1, a_2)$. The `rotate` operation is a relatively expensive operation, next to a `CMul` operation.

2.2.2 Scale Management Operations

RNS-CKKS further requires programmers to use the following scale management operations to meet the RNS-CKKS constraints (which are irrelevant to application algorithms).

Upscale: The `upscale` operation is a syntactic sugar (not a separate RNS-CKKS) operation that multiplies an operand ciphertext at scale m_1 with a multiplicative identity (*i.e.,* 1) at scale m_2, increasing the scale of the operand to $m = m_1 \cdot m_2$ (by an arbitrary amount). The operation can be used to match the scale of an addition operand if needed.

Modswitch (Figure 1d): The `modswitch` operation consumes one scale factor S_f without affecting the scale of a ciphertext, which in effect reduces the level by one. The operation can be used to adjust the level of an addition or multiplication operand if they do not match.

Rescale (Figure 1e): Multiplications accumulate the scales of ciphertexts. To avoid scale overflow (where the accumulated scale exceeds the maximum scale capacity ${S_f}^L$), RNS-CKKS supports the `rescale` operation that divides coefficient modulus Q by the scale factor S_f. In effect, the result's scale decreases from m to m/S_f (unlike `modswitch`) and its level decreases from l to $l-1$. Note that the `rescale` operation does not change the accumulated scale. To accommodate noises in RNS-CKKS operations, the `rescale` operation should be used only if the scale after rescaling still remains higher than the minimum scale waterline: *i.e.,* $m/S_f \geq S_w$.

Bootstrap (Figure 1f): Even with rescaling, for a program with a large number of multiplications, all available scale budgets will be eventually consumed and the accumulative scale will reach the cap. Further operations become infeasible due to a scale overflow. As a solution, RNS-CKKS supports the `bootstrap` operation that resets the scale and level of a ciphertext. After bootstrapping, the accumulated scale (and the current scale at level L) decreases to scale factor S_f. Table 2 shows the runtime latency of `bootstrap` from a different level to the maximum level L(=16). The `bootstrap` latency solely depends on the target level and does not depend on the level gap. As reported, `bootstrap` is the most expensive operation in RNS-CKKS: *e.g.,* 3774 times slower than `CAdd`, and 112 times slower than `CMul` at level 16.

3 Motivation

This section discusses the limitations of existing RNS-CKKS compilers and the difficulties in manual bootstrapping, motivating this work: new compiler support for bootstrapping.

3.1 Prior RNS-CKKS Compilers

Existing RNS-CKKS compilers [18, 41] aim to support automatic scale management that takes as input a program that consists of only arithmetic and rotation operations (implementing application computation logic), and inserts scale management operations `upscale`, `modswitch`, and `rescale` (but not `bootstrap`) to produce a new program that satisfies the RNS-CKKS constraints for security and correctness.

Although EVA [18] and Hecate [41] successfully automate many parts of scale management in RNS-CKKS, they both lack support for automatic bootstrapping management. As a result, they have been applied to relatively small deep-learning applications such as LeNet-5 [34], leaving more complex applications with a deep multiplicative depth out of reach.

3.2 Manual Bootstrapping Placement

Unfortunately, the state-of-the-art that supports large RNS-CKKS applications is manually adding `bootstrap` operations, which is error-prone and time-consuming. The manual placement is challenging for the following three reasons.

First, to avoid a scale overflow problem and ensure correctness, users should place a `bootstrap` operation before the accumulated scale (after the last bootstrapping) exceeds the maximum scale capacity ${S_f}^L$. Manually tracking the growth of the accumulated scales of a large number of ciphertexts is indeed very difficult because they depend on not only the existing arithmetic and rotation operations, but also newly added `upscale` or `rescale` operations for scale management.

Second, besides correctness, conducting performance-aware `bootstrap` operation placement manually (leading to lower latency) is even harder. As discussed earlier with Table 2, the `bootstrap` operation is much more expensive than any other operations. Thus, in most cases, it is a good idea to minimize the number of `bootstrap` operations (later we show that in some cases, more bootstrapping may count-intuitively lead to better performance).

Third, the bootstrapping placement affects scale management and its performance. The `bootstrap` operation changes the scale and level of a ciphertext (like other scale management operations), implying that the location of a `bootstrap` operation has a great influence on the level of the following ciphertexts, impacting the latencies of subsequent RNS-CKKS operations. For example, what should we do if we have multiple solutions with the same minimum number of `bootstrap` operations? Reasoning about the cascading impacts of multiple bootstrapping options is not a trivial task.

4 Key Observations and Insights

The RNS-CKKS compilers (*e.g.,* EVA [18] and Hecate [41]) can keep track of the scale and level of ciphertexts while placing scale management operations. A naïve compiler-based bootstrapping solution would be to extend them to place a `bootstrap` operation right before the RNS-CKKS operation that exceeds the maximum scale capacity (to avoid a scale overflow). However, we made two novel observations that such a naïve extension (based on an accumulated scale analysis) would lead to inefficient performance.

Observation 1: A simple accumulated scale analysis may introduce (unnecessarily) many `bootstrap` operations, incurring significant performance overhead. Consider a simple deep learning example in Figure 2a that consists of three convolution layers (`Conv1`, `Conv2`, and `Conv3`), two activation functions (`Act`), and one addition operation (`Add`). Figure 2a (right) shows ciphertexts (white box) and RNS-CKKS arithmetic and rotation operations (arrows). A simple convolution layer includes three pairs (channels) of one `Rot` and two `PMul` operations, aggregated by `CAdd` at the end. A simple activation function (`Act`) uses a single `CMul` operation.

Suppose that the scale of the input ciphertext x is 2^{40}, and its waterline, rescaling factor and the maximum scale capacity are 2^{40}, 2^{60} and 2^{300} (the initial level is 5). Figure 2b illustrates how the accumulated scale (left y-axis) and the level (right y-axis) of a ciphertext change in this example program (while scale management operations are omitted for simplicity). The x-axis reports the time latency, calculated using scaled profiled costs based on Table 2. Figure 2b shows the execution model of a naïve bootstrapping approach in which a `bootstrap` operation is added right before the RNS-CKKS operation that exceeds the maximum scale capacity. During the third `Conv3`, the accumulated scale would become larger than the maximum scale capacity on each of the three second `PMul` operations. To prevent scale overflow, the naïve compiler would add three `bootstrap` operations to reset the scales/levels of three ciphertexts Ms.

In Table 2, the `bootstrap` operation is much more expensive than any other operation. It is thus often profitable to use fewer `bootstrap` operations (if possible). The next two alternatives (analyzed by our compiler DaCapo) in Figure 2c and Figure 2d demonstrate that it is indeed possible to reduce the latency by placing fewer `bootstrap` operations at better locations. They are based on the following two key insights.

Insight 1A: A ciphertext liveness analysis can help reduce the number of `bootstrap` operations. Our first in-

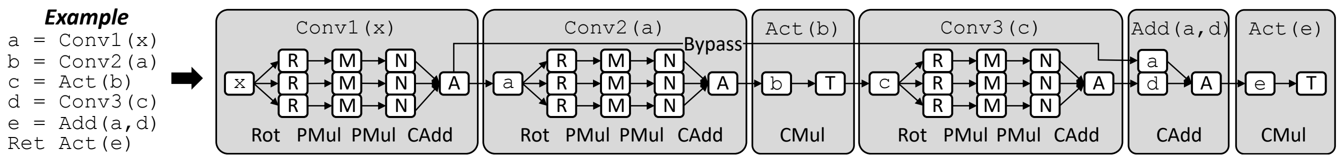

```
Example
a = Conv1(x)
b = Conv2(a)
c = Act(b)
d = Conv3(c)
e = Add(a,d)
Ret Act(e)
```

(a) Example program and its dataflow. The example consists of three convolution layers and two activation functions.

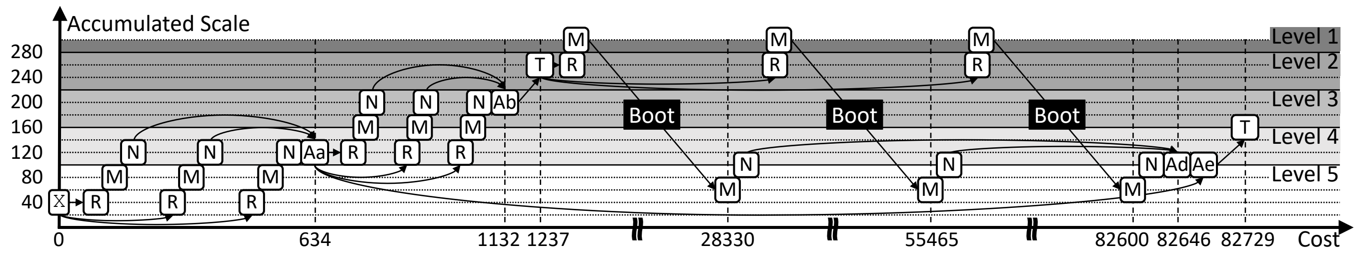

(b) Naïve approach. Bootstrapping is inserted right before the accumulated scale exceeds the scale capacity.

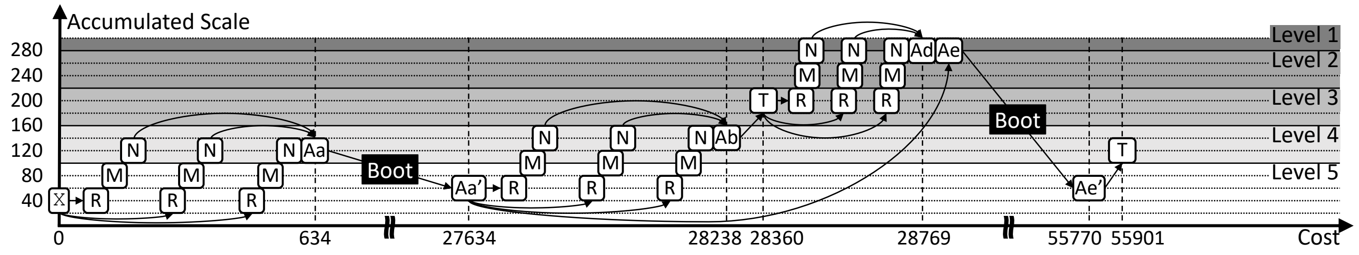

(c) Liveness-aware placement. Bootstrapping is inserted at the latest minimum live-out point before the accumulated scale exceeds the scale capacity.

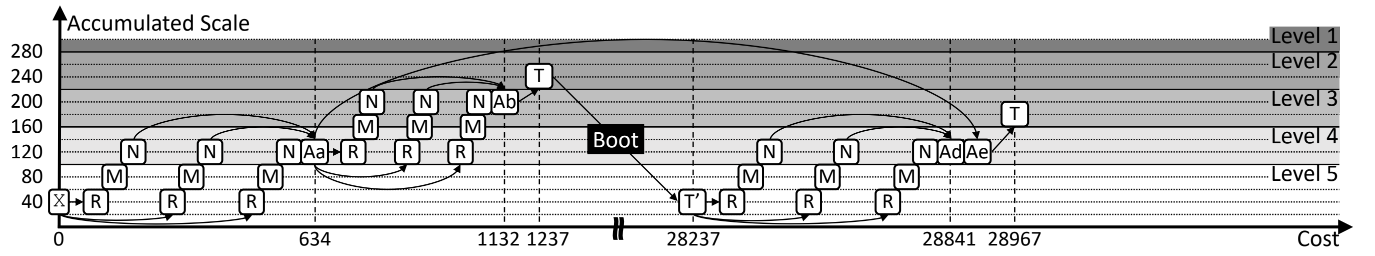

(d) Bypassed-liveness-aware placement. Bootstrapping is inserted in the same manner as liveness-aware placement but excluding bypass edges from the live-outs.

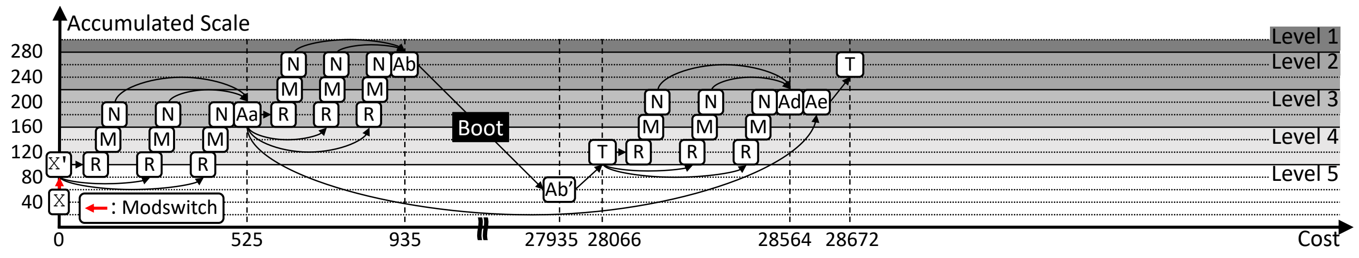

(e) Cost-aware placement (DACAPO). Bootstrapping is inserted at the best performance points among bypassed-liveness-aware candidates.

Figure 2: Motivating example and its execution models with different bootstrapping placement policies. The example assumes 2^{40} waterline, 2^{60} scaling factor, and 2^{300} scale capacity (the maximum level is 5).

sight is that the naïve approach added three `bootstrap` operations because a ciphertext dataflow diverges and three ciphertexts *M*s are later "used" so they all have to be bootstrapped for correctness. More formally in a compiler term, there were three *live-out* variables *M*s in a dataflow graph that must be bootstrapped. If the optimization goal is to minimize the number of `bootstrap` operations, then it would be beneficial to consider an alternative (and earlier) program point with fewer live-outs, or equivalently, a program point before a dataflow diverges or after it converges.

Based on this insight, DaCapo performs *liveness*-based bootstrapping management. More specifically, DaCapo counts the live-out ciphertexts at each program point, and regards minimum live-out points as candidate bootstrapping points. For instance, Figure 2c inserts the first `bootstrap` operation at the earlier program point with one live-out ciphertext *Aa* (after a dataflow converges from `Conv1(x)` and before it diverges to `Conv2(a)`), even though the accumulated scale is still much lower than the maximum capacity.

Insight 1B: A long-lived unused ciphertext that bypasses other RNS-CKKS operations is unlikely to require bootstrapping, so it is often profitable to exclude the ciphertext from the live-out counts. In a ciphertext dataflow graph (*e.g.,* Figure 2a), a bypass ciphertext implies the ciphertext that was defined but not used for a while. For instance, the ciphretext *A* is defined at the end of the `Conv1(x)`; not used by (bypassing) `Conv2(a)`, `Act(b)`, and `Conv3(c)`; and finally used by `Add(a,d)`. The long-lived ciphertext is represented as a long edge from *A* in `Conv1(x)` to *a* in `Add(a,d)`. Such a long-lived unused (bypass) ciphertext is unlikely to require `bootstrap`. A strict inclusion of those ciphertexts in liveness analysis may unnecessarily increase live-out counts at some program points, and remove bootstrapping placement candidates, thus losing further optimization opportunities. Then, DaCapo would not consider those program points as bootstrapping candidates.

To address them, DaCapo excludes the long-lived (unused-for-a-while) ciphertexts from the live-out counts, achieving better bootstrapping management. For example, consider the ciphertext *T* in `Act(b)`. At that program point, the actual live-out count is two including the short edge from *A* in `Conv1(x)` to *b* in `Act(b)`, and the bypass edge from *A* in `Conv1(x)` to *a* in `Add(a,d)`. The plain liveness-based DaCapo would not consider the program as bootstrapping candidates and produces the bootstrapping result in Figure 2c. On the other hand, once the bypass edge is excluded, the new live-out count will be one. DaCapo could find a better plan in Figure 2d with only one `bootstrap` operation.

Observation 2: Different bootstrapping placements (locations and numbers) may lead to widely different end-to-end latency because bootstrapping may allow other RNS-CKKS operations to be performed at lower levels. As the `bootstrap` operation resets the scale and level of a ciphertext, adding one `bootstrap` in effect can be viewed as partitioning a given program into two smaller sub-programs. Interestingly, if one partition has fewer multiplications (less multiplicative depth), the arithmetic and rotation operations in that partition may be executed at lower levels, resulting in less end-to-end latency. Note that RNS-CKKS operations run faster at lower levels (See Table 2). For the same reason, we also make a rather counter-intuitive observation that fewer `bootstrap` operations do not always lead to lower latency. More `bootstrap` operations imply more partitioning of a given program. Each partition would have fewer operations, which can be performed at lower levels, resulting in less latency. The performance improvement with lower-level operations may be greater than the performance overhead of additional `bootstrap` operations.

Insight 2: A cost-aware bootstrapping analysis is needed for performance. Learned from the above observation, DaCapo leverages the aforementioned liveness analysis to collect different bootstrapping candidates, and compares static cost (latency) estimates among them to select the lowest. For example, compare two different bootstrapping locations between Figure 2d and Figure 2e for the same number (one) of `bootstrap` operations. Figure 2e performs bootstrapping before `CMul` in `Act(b)`, allowing many arithmetic and rotation operations in the first partition (the ones in `Conv1(x)` and `Conv2(a)`) to be performed at level 4 or less after early `modswitch` (shown in a red arrow). On the other hand, Figure 2d performs many of these operations at a higher level 5, leading to higher end-to-end latency.

5 Overview

This work proposes DaCapo, the first FHE compiler that automatically places `bootstrap` operations. Given an input program written in plain operations, DaCapo transforms the plain operations into RNS-CKKS operations with scale management operations including `bootstrap`, and generates LLVM IR codes that invoke GPU-accelerated HEaaN library [25] for RNS-CKKS operations. To support cost-aware bootstrapping placement, DaCapo consists of two components: candidate selector and bootstrapping planner. Figure 3 shows DaCapo's two-step workflow on the left along with an example on the right side, which will be explained later.

Candidate selector identifies candidate points in the program where bootstrapping can be inserted. The candidate selection consists of three steps: liveness analysis, bypass edge analysis, and candidate filtering. The *liveness analysis* step analyzes live-out ciphertexts at each program point, and the *bypass edge analysis* step analyzes long-lived unused edges like the edge from *A* in `Conv1(x)` to *a* in `Add(a,d)` in Figure 2a. Combined, the candidate selector can analyze the number of valid live-out ciphertexts that may need bootstrapping at each program point. The *candidate filtering* step finalizes the candidate points. If the candidate points are too few to generate a correct FHE program due to scale overflow, the candidate filtering step increases the threshold number of live-outs until the scale overflow is resolved.

DaCapo's bootstrapping candidate program points selection implies that it adds `bootstrap` operations synchronously to all the live-out ciphertexts except for bypass ones at those program points. If a compiler bootstraps only a subset of live-out ciphertexts that needs to be refreshed (*i.e.,* not all at once), chances are that the refreshed accumulated scale may be wasted because of the level match constraints of RNS-CKKS arithmetic operations. When the levels of two addition or multiplication operands are different, a scale management

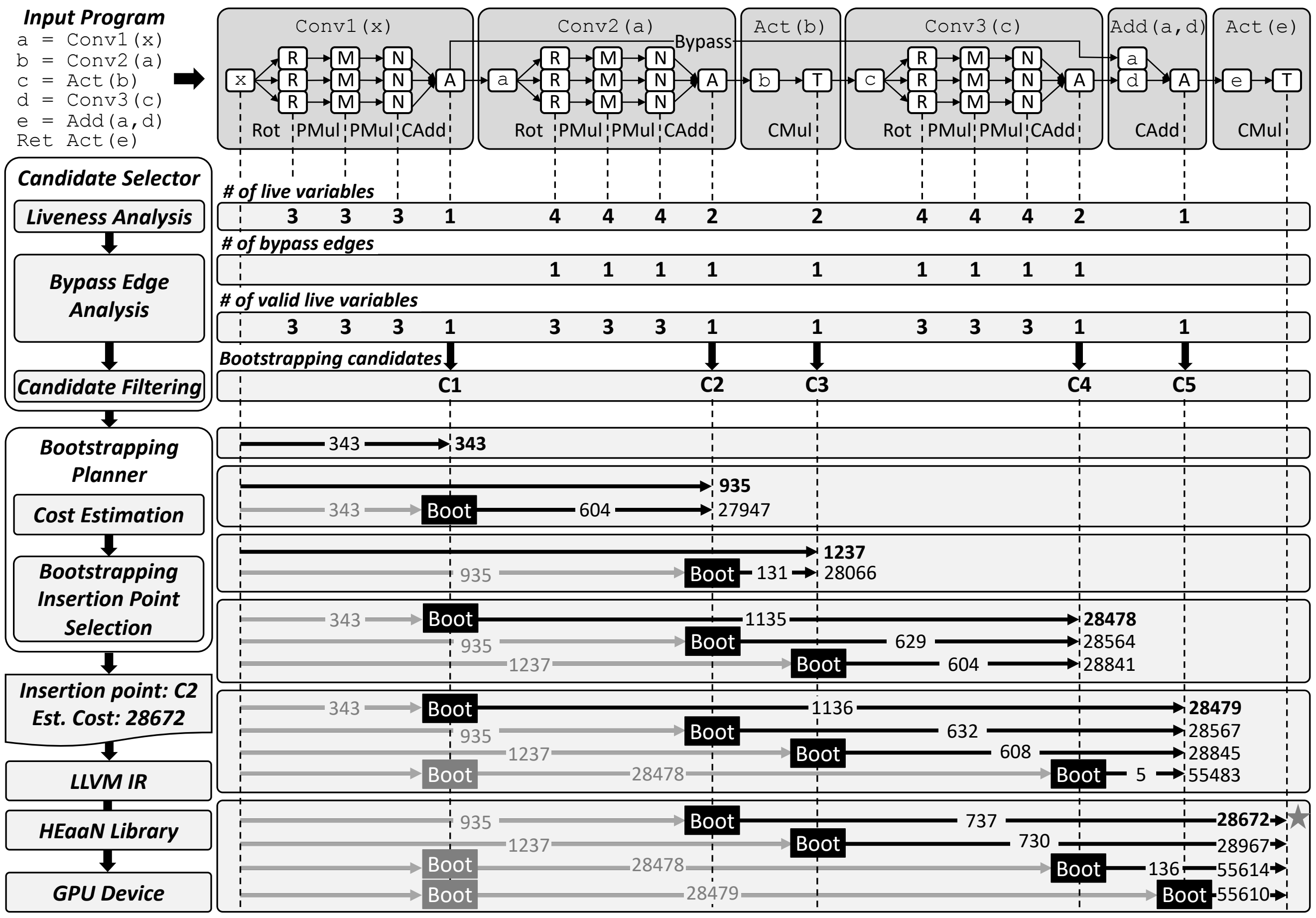

Figure 3: Overview design of DACAPO with the example in Figure 2a. Candidate selector analyzes live-outs and bypass edges, and identifies candidate points where bootstrapping can be inserted. Bootstrapping planner estimates computation costs at each candidate point, and determines the bootstrapping insertion points with minimum overall latency among the candidate points. The bold numbers at the end of each candidate indicate the minimum computation cost. Gray arrows and numbers are the best estimated costs at the bootstrapping insertion point computed in the previous steps. The star indicates the selected plan.

scheme uses `modswitch` to match them to the smaller level. If not all live-outs are bootstrapped, this implies the just refreshed (bootstrapped) accumulated scale may be increased to the stale one to be used for following arithmetic operations. DACAPO avoids such a bootstrapping waste.

Bootstrapping planner computes the costs of RNS-CKKS operations and, determines the bootstrapping placement plan with minimum overall latency among the candidate insertion points from the candidate selector. The bootstrapping planner consists of two steps: cost estimation and bootstrapping insertion point selection. The *cost estimation* step estimates the latency at each candidate point using profiled RNS-CKKS operation costs. Since RNS-CKKS operations have different costs at different levels, this step implicitly executes scale management from the last bootstrapping points to the current candidate points. Among the estimated costs, the *bootstrapping insertion point selection* chooses the plan with the minimal costs, and finalizes the bootstrapping placement plan.

6 Bootstrapping Candidate Selector

This section introduces the bootstrapping candidate selector with an algorithm that analyzes appropriate candidates for bootstrapping placement. The candidate selector analyzes the live-out of each program point via liveness analysis, and identifies the required number of `bootstrap` for each program point by excluding bypass edges (§6.1). Then, the candidate selector finalizes the candidates from the candidate sets grouped by the number of `bootstrap` (§6.2).

6.1 Liveness and Bypass Edge Analysis

Liveness and bypass edge analysis find all the ciphertexts that should be bootstrapped if DACAPO decides to insert `bootstrap` at a program point. With the liveness analysis, DACAPO can find all the live-out ciphertexts that will be used later at a certain program point (*LiveVariable* in Algo-

Algorithm 1: Bootstrap Candidate Selection

```
   Input: Func: Function of an HE application
   Output: Set: Set of candidates
1  Function CandidateSelector (Func) :
2      // Bypass Edge Analysis (Section 6.1)
3      BypassEdges, CandidatesSet ← {}
4      foreach target ∈ Func do
5          BootTarget ← LiveVariable(target) − BypassEdges
6          CandidatesSet[BootTarget.size] += target
7          Managed ← ScaleManagement(Func, target)
8          foreach op ∈ Managed after target do
9              if op.AccumulatedScale > $S_{th}$ and
10                 EndOperation(target) after op then
11                 BypassEdges += {target}
12             if op.AccumulatedScale > ${S_f}^L$ then
13                 target.Coverage ← op
14                 break
15         end
16     end
17     // Candidate Filtering (Section 6.2)
18     threshold ← 1
19     Candidates ← CandidatesSet[threshold]
20     while not success do
21         success ← true
22         Managed ← ScaleManagement(Func, Candidates)
23         foreach op ∈ Managed do
24             if op.AccumulatedScale > ${S_f}^L$ then
25                 threshold += 1
26                 Candidates += CandidatesSet[threshold]
27                 success ← false
28         end
29     end
30     return Candidates
31 end
```

rithm 1), and the last program point where the ciphertext is used (*EndOperation* in Algorithm 1). The bypass edge analysis finds ciphertexts that are live but not used during a long computation (that the accumulated scale exceeds the threshold S_{th}), and excludes them from the required bootstrapping counts at a certain program point.

Algorithm 1 illustrates the algorithm for the bootstrapping candidate set generation. First, the algorithm performs bypass edge analysis (line 2-16). For each program point (`target`) in a function, the algorithm analyzes `bootstrap`-required ciphertexts by removing bypass edges from the live-outs (line 5), and adds the `target` into a candidate set with the same number of the required `bootstrap` operations (line 6). Then, the algorithm checks if the result ciphertext of the operation at `target` includes bypass edges, and calculates the coverage of `bootstrap` at `target`. Assuming that `bootstrap` is inserted at the `target`, the algorithm executes scale management on the given function using the proactive rescaling scheme of Hecate [41] (line 7). The algorithm categorizes the result of the operation at `target` as a bypass ciphertext if the result is live after an operation whose accumulated scale exceeds the threshold S_{th} (line 9-11). Furthermore, the algorithm checks the accumulated scale of operations in *managed* and identifies the operations that can be executed without additional `bootstrap` (line 12-14). The remaining algorithm will be explained in §6.2.

Figure 3 illustrates how the liveness and bypass edge analysis analyze the example program. First, the liveness analysis gives the number of live variables for each program point. For example, there are 3 live variables (3 Rs) after `Rot` in `Conv1`. Note that this analysis counts the live-out variables, not the uses of the variables, so there is 1 live variable after `Conv1`. Then, the bypass edge analysis detects and removes a bypass edge from the live-out variable sets. For example, Aa in `Conv1` is live-out until `Add`, but the accumulated scale of Ad in `Conv3` before `Add` is 280 (see Figure 2c) that exceeds the threshold S_{th} (*e.g.,* 180). Therefore, the analysis classifies Aa as a bypass edge and then removes Aa from the live variable set of other operations. Then, the number of live variables after Ab (`Conv2`) is reduced from 2 ($\{Aa, Ab\}$) to 1 ($\{Ab\}$).

The S_{th} value, which is heuristically determined by users, impacts the performance of the generated code. A higher S_{th} makes Algorithm 1 detect fewer bypass edges, thus causing DACAPO to insert unnecessary bootstrapping operations for long-lived unused ciphertext. On the other hand, a lower S_{th} makes Algorithm 1 mark more edges with a shorter life-span as bypass edges, so DACAPO may exclude edges requiring bootstrapping from the candidates. Thus, assigning an appropriate S_{th} value is crucial for optimizing the bootstrapping placement. This work uses S_{th} as half of the maximum scale capacity for the evaluation.

6.2 Candidates Filtering

DACAPO generates a candidate set by filtering the bootstrapping targets based on the number of `bootstrap`. If the scale management cannot generate a valid program for a given candidate set, meaning that the accumulated scale of a ciphertext exceeds its scale capacity, the given candidate set needs to be expanded. On the other hand, to minimize the number of `bootstrap`, the algorithm should find the minimal threshold of filtering. Hence, to find the minimal filtering threshold, the candidate filtering gradually increases the threshold from 1 to a value that can generate a valid scale management plan.

Line 17-29, describe the candidate filtering algorithm. The algorithm initializes the candidate set with targets requiring only one `bootstrap` (line 19). The algorithm executes scale management for the candidate set (line 22), and checks if the accumulated scale of a ciphertext exceeds the scale capacity. If so, the algorithm increases the threshold and expands the candidates (line 23-27). If the filtering is finished, the algorithm returns the finalized `bootstrap` candidate set (line 30).

Figure 3 illustrates how the candidate filtering works for the

Algorithm 2: Bootstrapping Planner Algorithm

```
Input: Set: Candidates
Output: Set: Bootstrapping Targets
Function BootstrappingPlanner (Func, Candidates):
    Candidates.push (Func.ReturnOp)
    foreach to ∈ Candidates do
        foreach from ∈ Candidates do
            if to before from.Coverage then
                Managed ← ScaleManagement (Func,
                        BestPlan[from] + to)
                cost ← EstimateCost (Managed, from, to)
                cost ← cost + MinCost[from]
                if cost < MinCost[to] then
                    MinCost[to] ← cost
                    BestPlan[to] ← BestPlan[from]
                    BestPlan[to] += to
        end
    end
    return BestPlan[ReturnOp]
end
```

example. First, the candidate filtering algorithm only considers the bootstrapping candidate set ($\{C1, C2, C3, C4, C5\}$) that has only one valid live variable $\{Aa, Ab, T, Ad, Ae\}$, respectively. For the candidate set, the algorithm inserts `bootstrap` for each candidate and then performs scale management. If there is no operation whose accumulated scale exceeds the scale capacity, the candidate set is valid. If the candidate set is not valid, the algorithm increases the threshold number of valid live variables to expand the candidate set.

7 Cost-aware Bootstrapping Planner

This section describes the bootstrapping planner that finds bootstrapping insertion positions with minimal latency costs, for the given bootstrapping placement candidates from bootstrapping candidates selection (§6). Since `bootstrap` operation resets the scale and level of a ciphertext, depending on the bootstrapping placement, the scale management results vary, and thus the latency (level) of each ciphertext varies also. To optimize the bootstrapping placement plan reflecting the varying latency, the bootstrapping planner estimates the cost for each candidate and decides the placement plan with minimum overall cost. Here, this work employs a simple cost estimation that adds the profiled latency of each RNS-CKKS operation (*e.g.,* Table 2).

Algorithm 2 illustrates the bootstrapping placement plan decision algorithm. For each *to* candidate, the algorithm analyzes the minimum estimated cost from the beginning of the program to the *to* program point. Iterating other *from* candidates before *to*, the algorithm executes scale management from *from* to *to*, estimates its latency cost, adds the estimated cost and the minimum cost at *from*, and finds the minimum cost by comparing the added result with the existing minimum estimated cost at *to*. Note that the scale management result is memorized while not reflected in the algorithm. Since the scale management of subprograms before and after `bootstrap` is decoupled, and the input scale and level of the succeeding subprogram only depend on `bootstrap`, the minimum cost can be computed by adding the current estimated cost and the minimum cost at *from*. The algorithm returns the bootstrapping plan at *ReturnOp* as the final placement plan.

Figure 3 illustrates how the bootstrapping planner algorithm works in the example. First, the planner executes scale management and estimates the cost of the partial program. For example, the planner estimates the cost of a partial program until $C1$ as 343. Then, to find a bootstrapping placement plan with the minimal estimated cost until the next candidate $C2$, the planner considers two different cases. For the case that `bootstrap` is not inserted at $C1$, the planner estimates the cost (935) in the same way as $C1$. For the case that `bootstrap` is inserted at $C1$, the planner reuses the previous estimation result for $C1$ (343), and adds the latency of `bootstrap` (27000) and the latency of the partial program from $C1$ to $C2$ (604), calculating the resulting cost (27947). The planner compares the estimated costs of two cases and selects the lower one (no `bootstrap`). The selected plan for $C2$ is reused for the other candidates such as $C3$, $C4$, $C5$, and *Ret*.

8 Evaluation

The evaluation section first describes our experimental setup in §8.1 and demonstrates the overall performance improvement of DaCapo compared to manually implemented programs in §8.2. We also show the effectiveness of DaCapo by comparing the bootstrapping counts in §8.3, and highlight its practicality by analyzing the compile time in §8.4. Furthermore, we present the accuracy of performance estimation in §8.5. Lastly, we perform the latency sensitivity study with varying waterlines for each benchmark application in §8.6.

8.1 Experimental Setup

This paper evaluates multiple complex deep learning models with two different activation functions, including ResNet-20/44 [24], AlexNet [31], VGG16 [49], SqueezeNet [29], and MobileNet [27]. ResNet-20 was initially introduced as a HE-friendly model in [38], and we use the improved versions of ResNet-20/44 presented in [36]. The activation functions were implemented based on the algorithm proposed in [37]. In detail, we use the Remez algorithm to approximate SiLU as a 96th-order single polynomial (multiplicative depth of 7). On the other hand, ReLU employed a minimax composite polynomial approximation using degrees {15, 15, 27} (multiplicative depth of 13) in [37]. For linear operations such as convolution, we adopt the multiplexed parallel convolution

Table 3: Classification accuracy for multiple CIFAR-10 images using models on the RNS-CKKS scheme generated by DACAPO.

Model	ResNet-20		ResNet-44		AlexNet		VGG16		SqueezeNet		MobileNet	
	ReLU	SiLU	ReLU	SiLU	ReLU	SiLU	ReLU	SiLU	ReLU	SiLU	ReLU	SiLU
Pytorch	90.6%	92.6%	91.2%	92.7%	89.0%	86.6%	93.8%	93.0%	89.4%	88.0%	91.4%	91.4%
DACAPO	90.7%	92.6%	91.3%	92.7%	89.0%	86.6%	93.8%	92.9%	89.2%	87.9%	91.2%	91.4%

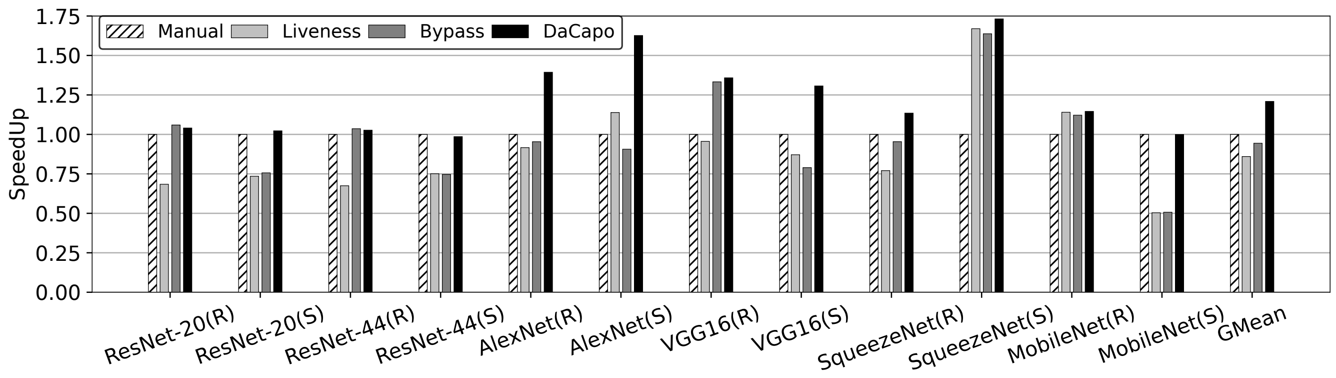

Figure 4: Speedup of algorithms based on the Manual with waterline 2^{40}. The activation functions utilized in each deep learning model are denoted as (*R*) for ReLU and (*S*) for SiLU.

technique introduced in [36], which enables the compact representation of sparse output data across multiple channels. The evaluation includes a total of 12 benchmark results, considering two activation functions and pooling layers: ReLU with max pooling (R), and SiLU with average pooling (S).

We implemented the above deep learning benchmark applications using a GPU-accelerated RNS-CKKS library HEaaN [25]. To facilitate development, we implemented common neural network operators such as convolution (`Conv`) and activation functions ReLU and SiLU on the RNS-CKKS scheme.

We validate our implementation by comparing the accuracy using 1,000 CIFAR-10 images between PyTorch's and the DACAPO programs (with a waterline of 2^{40}). Table 3 reports the classification accuracy results. ResNet-20(R), SqueezeNet(R) and (S), and MobileNet(R) exhibited a minor difference of 0.1% in accuracy. The usage of approximate activation functions introduced a maximum error of 13 bits, leading to negligible differences in accuracy.

Given the lack of bootstrapping compilers, our evaluation uses manually implemented bootstrapping placement (**Manual**) as the baseline. According to the state-of-the-art ResNet-20/44 implementation with bootstrapping [36], which inserts `bootstrap` operations before activation functions only when deemed necessary, we manually insert bootstrapping operations for the benchmark applications. The manual insertion, verification, and optimization take approximately 4 hours for each benchmark for a single waterline. Since an incorrect placement of bootstrapping causes FHE operation errors such as ciphertext scale overflow, sophisticated time-consuming placement analysis and verification are required. For this version, `bootstrap` operations are added between each layer. In addition, the sign function used in ReLU and maxpooling cannot be executed without bootstrapping, so we incorporate additional bootstrapping at the point where the second 15th-degree term is multiplied. The manual implementation assumes a scale management waterline of 2^{40}.

We compare DACAPO's three different variants with the manual implementation (**Manual**). **Liveness** only considers the number of live-out values at program points (without bypass edge or cost analysis). This method greedily utilizes the scale budget in that it inserts `bootstrap` synchronously while maximizing the utilization of the scale capacity by inserting `bootstrap` into the closest candidates when the accumulated scale exceeds the scale capacity. Figure 2c represents this scheme. **Bypass** considers more `bootstrap` candidates by excluding the bypass edges. Like Liveness, it greedily maximizes the scale capacity utilization but does not perform cost-aware bootstrapping. Figure 2d is an example of this scheme. **DACAPO** use all the proposed liveness, bypass, and cost analyses, as illustrated in Figure 2e. It regards the latency of all operations and determines the placement of `bootstrap` based on the bypass-aware candidates set.

This evaluation runs on Intel(R) Core(TM) i7-12700 for CPU and NVIDIA GeForce RTX 3090 with 24GB memory for GPU, utilizing unified virtual memory (UVM).

Table 4: Bootstrapping counts for each benchmark in manual placement and DaCapo

Model	ResNet-20		ResNet-44		AlexNet		VGG16		SqueezeNet		MobileNet	
	ReLU	SiLU	ReLU	SiLU	ReLU	SiLU	ReLU	SiLU	ReLU	SiLU	ReLU	SiLU
Manual	37	19	85	43	66	12	54	20	58	18	53	27
DaCapo	37	19	85	43	67	12	53	20	57	19	61	27

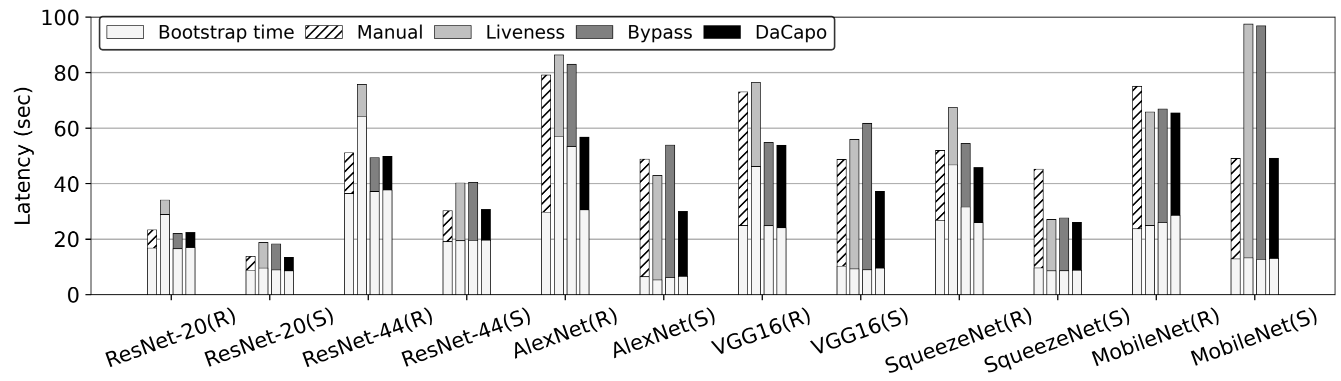

Figure 5: Inference time for a single image. The white portion of bar represents the latency introduced by bootstrapping.

8.2 Performance Evaluation

Figure 4 represents the speedup of inference time for a single CIFAR-10 image achieved by each approach (Liveness, Bypass, and DaCapo) compared to Manual.

In Figure 4, Liveness allows for effective reduction of # `bootstrap`, which achieves comparable performance to Manual in VGG16(R) and VGG16(S), and even improves the performance in cases like AlexNet(S) and SqueezeNet(S). The main reason Liveness improves the performance is that the compiler considers the bootstrapping points the user cannot consider, such as the points within an activation function. Bypass increases the number of valid liveness candidates, finding more beneficial `bootstrap` candidates. In ResNet-20/44(R) and VGG16(R), improved latencies can be observed by identifying appropriate points considering liveness. However, in the case of VGG16(S) and AlexNet(S), the total latency actually increases as shown in Figure 5, due to increased latencies in other operations. The geometric mean of speed up for DaCapo is $1.21\times$. The reason why DaCapo achieves better results compared to Manual is that DaCapo takes into consideration the aspects that users may overlook. DaCapo has the ability to analyze the detailed RNS-CKKS operations that make up deep learning model APIs. While users can analyze the provided library and insert `bootstrap`, due to the variability of scale management with each function call, the optimal point for `bootstrap` can vary each time. DaCapo, on the other hand, is aware of scale management variations based on the placement of `bootstrap`, allowing it to discover a lower latency plan than Manual.

8.3 Bootstrapping Counts

In Table 4, the number of `bootstrap` operations is similar between Manual and DaCapo. However, in Figure 5, DaCapo yields apparently better latency for AlexNet, VGG16, and SqueezeNet because DaCapo places the bootstrapping where the latency of arithmetic is reduced. Interestingly, in the case of MobileNet, DaCapo involves a higher number of `bootstrap` operations, yet it still achieves a lower total latency. This is strong evidence that the latency of arithmetic operations has an impact on the overall latency, although each arithmetic operation has multiple orders lower latency than bootstrapping. In the case of MobileNet(R), there are a large number of channels leading to increased `rotate` and multiplication operations, which outweigh the latency of `bootstrap`, increasing the number of `bootstrap` operations can actually result in a lower total latency by lowering the levels of intermediate operations. This demonstrates that simply minimizing the `bootstrap` count does not guarantee optimal results.

8.4 Compile Time

Table 5 shows the total compile time and bootstrapping management time for each benchmark, along with a comparison of the number of operations and `bootstrap` candidates. Benchmarks with ReLU have more candidates because the composite polynomial approximation of ReLU has multiple points with a single live-out. For all the benchmarks except AlexNet, the management time is less than 5 minutes, which is acceptable as usual. To discuss the scalability of the algorithm, we perform an in-depth analysis of the compile time.

Table 5: Compile time and bootstrapping management time by DaCapo on the RNS-CKKS scheme (sec)

Model	ResNet-20		ResNet-44		AlexNet		VGG16		SqueezeNet		MobileNet	
	ReLU	SiLU	ReLU	SiLU	ReLU	SiLU	ReLU	SiLU	ReLU	SiLU	ReLU	SiLU
# Ops	8784	9144	19412	20204	53533	50535	45798	44766	21404	19264	44919	45411
# Candidates	138	100	306	220	662	95	166	71	251	52	191	136
Compile Time (s)	33.0	31.0	116.5	109.2	1163.8	454.0	332.7	290.2	131.2	84.8	302.3	302.1
Bootstrap Mgmt. Time (s)	15.8	14.4	79.4	72.8	1042.3	336.5	230.1	188.1	89.1	44.1	222.8	218.0

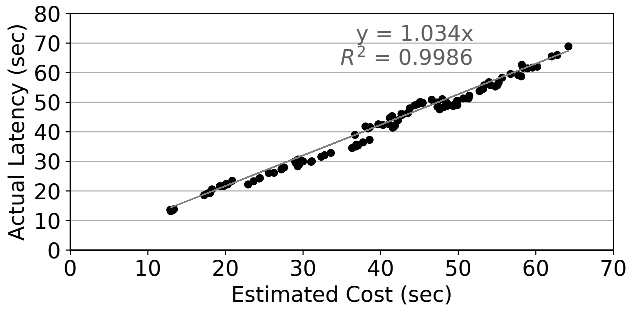

Figure 6: Precision of the estimation results. The x-axis represents the estimated results by DaCapo based on profiled data, and the y-axis indicates actual latency.

In bootstrapping management, time-consuming parts are bypass edge detection and the bootstrapping plan decision. The bypass edge detection algorithm, which calculates coverage through scale management for each operation, has a time complexity of O(N^2), where N is the number of operations. On the other hand, Algorithm 2 has a time complexity of O($D \times d \times N$), where D is the number of `bootstrap` candidates and d is the maximum number of `bootstrap` candidates within the coverage of a certain `bootstrap` candidate.

Comparison between the ResNet-20(S) and the AlexNet(S) shows the impact of the number of operations on the bypass edge detection clearly ($(50535/9144)^2 = 30.54$ vs $336.5/14.4 = 23.37$). The scale management unit [41] will greatly reduce the effective number of operations, enhancing its scalability. On the other hand, the comparison between AlexNet(R) and AlexNet(S) clearly shows the impact of the number of candidates on the plan decision algorithm. Since the intermediate feature maps cannot be packed in a single ciphertext in AlexNet(R), the candidate filtering threshold is larger than other benchmarks, increasing candidates a lot. We believe that further research on a fine-grained filtering threshold that reflects the program context can improve the scalability of the plan decision algorithm.

8.5 Performance Estimation

To evaluate the accuracy of the latency estimation used in Algorithm 2, we compared the estimated latency with the actual latency with 108 data points using 12 benchmarks across 9 different waterlines in Figure 6. The equation, $y = 1.034x$, is a regression model between the estimated and actual costs, and R^2 indicates predicted latency closely aligns with the actual latency. Since the coefficient of the regression model and the R^2 value (0.9986) are close to 1, the overall precision is quite satisfactory. The small variances in the coefficient and R^2 are caused by the memory transfer latency in UVM. We use a GPU that has 24GB of physical RAM, whereas the memory requirement exceeds the capacity in some benchmarks. Therefore, UVM was used for the experiment to fulfill the memory usage, which might have imposed an additional latency to the actual execution time compared to the estimated time in the memory-starving benchmark. Nonetheless, the variance in the performance estimation will not degrade the efficacy of the bootstrapping plan decision, because the penalty of memory starvation will affect the bootstrapping placement plans of the same benchmark consistently.

8.6 Waterline Sensitivity

Figure 7 illustrates the latency for deep learning benchmarks with respect to the waterline. The approximation of the activation function has a maximum 13-bit error. To align the error caused by RNS-CKKS operations with the approximation error of activation functions, the waterline needs to be larger than 2^{30} in our measurement. The latency of Manual is plotted as a point based on a waterline of 2^{40}. A lower waterline gives a different scale management plan that slows down the scale accumulation, leading to different optimal positions for bootstrapping placement. Greedy bootstrapping placements (Liveness and Bypass) can find reasonable positions as observed in ResNet-20 and SqueezeNet but result in a significant variance of latency for AlexNet and MobileNet, because the position of `bootstrap` significantly changes the latency of arithmetic operation. On the other hand, DaCapo exhibits lower variation with respect to the waterline and shows a decreasing trend of total latency as the waterline decreases. For Figure 7k, there is a small variance depending on the waterline. The variance comes from the scale management scheme (the proactive rescaling of Hecate) that does not optimize the latency of arithmetic operation consistently and produces sub-optimal scale management plans. Hecate [41] conducts

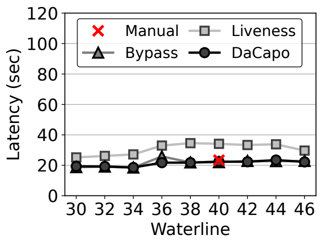

(a) ResNet-20 (ReLU)

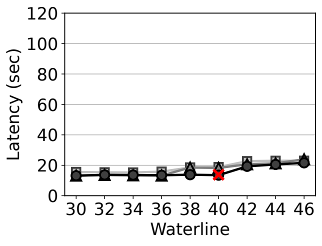

(b) ResNet-20 (SiLU)

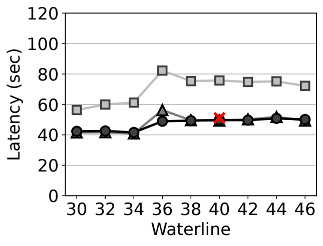

(c) ResNet-44 (ReLU)

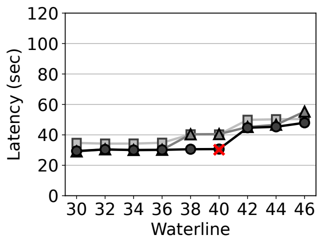

(d) ResNet-44 (SiLU)

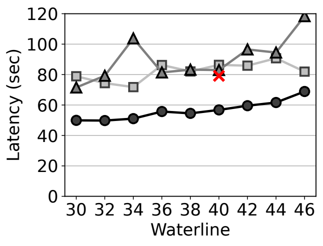

(e) AlexNet (ReLU)

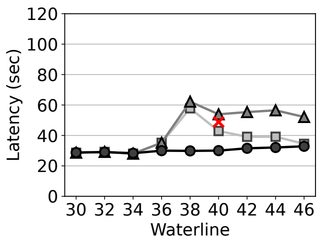

(f) AlexNet (SiLU)

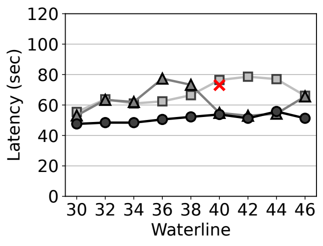

(g) VGG16 (ReLU)

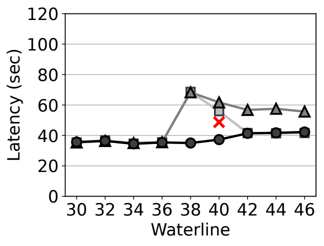

(h) VGG16 (SiLU)

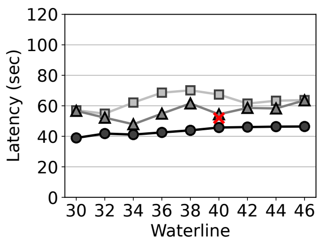

(i) SqueezeNet (ReLU)

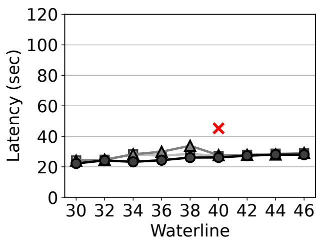

(j) SqueezeNet (SiLU)

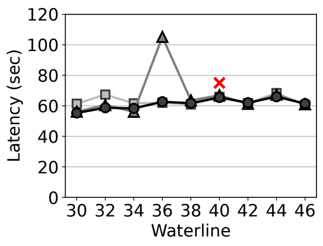

(k) MobileNet (ReLU)

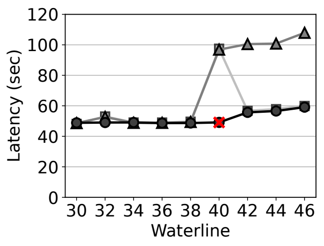

(l) MobileNet (SiLU)

Figure 7: The latency of each benchmark corresponding to different waterlines (lower is better). Manual results are represented by one point based on waterline 2^{40}.

space exploration to find the optimal points but requires significantly longer compile time due to the larger benchmark size. Further improvement on the scale management scheme could lead to improvements in this aspect.

9 Related Work

FHE compilers. The existing compiler works [4–6, 9, 13, 15, 18, 19, 35, 39–41, 43, 50, 51, 53], have proposed optimization techniques to improve performance, accuracy, and programmability. EVA [18] introduces the concept of *waterline* which signifies the minimum required scale and automates inserting scale management operations. However, EVA misses the opportunity for optimization as it uses fixed-factor rescale. To address the limitation of EVA, HECATE [41] proposes downscale operation which enables proactive rescale and finds an optimal scale management plan by using space explorations. ELASM [39] points out that using a fixed waterline in HE applications does not reflect errors during scale management. With a new error-latency-aware scheme, ELASM produces better latency and error results than prior works [18,41].

DACAPO and the existing compilers such as Hecate and ELASM have complementary relations. This work focuses on how to partition DNN models using bootstrapping, while the other compilers focus on scale management optimization of each partition. The bootstrapping management algorithm of DACAPO can be applied in conjunction with any scale management scheme. However, simply applying Hecate or ELASM to this work is impractical due to their high exploration overheads. Hecate and ELASM optimize ciphertext scales by exploring scale management spaces, and scale management space exploration takes huge compilation overheads. Since DACAPO generates multiple different bootstrapping insertion candidates, and optimizes ciphertext scales that are reinitialized at each bootstrapping insertion point, exploration-base scale management like Hecate and ELASM would severely amplify the compilation time. Thus, this work adopts only a part of Hecate such as the proactive rescaling scheme to manage ciphertext scales, while excluding the scale management space exploration from Hecate.

In addition, performance improvement is achieved through effective data layout and parallelization methods for ciphertexts. CHET [19] automatically selects the encryption parameters and data layout while ensuring security and accuracy of the target tensor circuit. EVA [18] and ALCHEMY [16] also provide data packing, but still lacks usability as programmers have to perform vectorization manually. Coyote [43] allows automatic vectorizing for arbitrary applications considering data movement. HECO [50] incorporates circuit optimizations to reduce noise growth, as well as target hardware and scheme-specific optimizations, enabling developers to achieve performance similar to experts. However, none of the compilers support large benchmarks that require bootstrapping.

Privacy Preserving Machine Learning (PPML). A Convolution algorithm for homomorphic encryption is proposed by Gazelle [30], and [3,28,32,44,47,52] perform Convolution Neural Network (CNN) based on this algorithm. These works adapt multi-party computation to perform non-linear functions on secure side, which compromised the advantages of homomorphic encryption and required significant communication overhead. [38] first implements the standard ResNet-20 with the RNS-CKKS FHE with bootstrapping, but a substantial amount of bootstrapping operations and convolutions lead to performance degradation. To improve the efficiency of the application, [36] constructs an efficient very deep standard CNN model on FHE, which minimized the bootstrapping runtime by applying multiplexed packing and multiplexed parallel convolution algorithm. All existing PPML are hand-optimized and do not reflect scale management. Additionally, programmers need to manually insert bootstrapping for each change in waterline and model structure, which increases their burden and might create target programs inefficiently.

Automatic Bootstrap Placement. Previous work [45] proves that finding the minimal number of `bootstrap` for a given FHE program and corresponding bootstrapping placement is an NP-complete problem. They propose heuristics for bootstrapping placement based on a mixed-integer linear programming method. Compared to DaCapo, they only consider the multiplicative depth not reflecting scale management, and do not consider the latency of the other operations. Furthermore, they do not automatically generate the `bootstrap`-managed code to reduce the programming burden.

This work proposes an automatic bootstrapping management compiler to reduce the burden on developers and enable easy privacy-preserving use of large-size models. Also, the results show improved performance to manual-implemented models and demonstrate the minimum number of bootstrapping counts does not always result in better performance.

10 Conclusion

This paper introduces DaCapo, which is the first automatic bootstrapping management compiler. DaCapo efficiently restricts bootstrapping candidates through liveness analysis, considering bypass edges. Additionally, DaCapo finds the bootstrapping plan with the minimum cost based on these candidates. The results demonstrate that DaCapo consistently outperforms manually implemented FHE programs on deep learning models, achieving an average speedup of 1.21×.

Acknowledgements

We appreciate the valuable feedback and shepherding from anonymous reviewers and the support from CoreLab members during this work. This work is partly supported by IITP-2020-0-01847, IITP-2020-0-01361, IITP-2021-0-00853, IITP-2022-0-00050, and No. RS-2023-00277060 funded by the Ministry of Science and ICT, South Korea. This work is also supported by Samsung Electronics and CryptoLab. This work is in part supported by the grants CNS-2135157, CCF-2153747, and CNS-2214980, funded by the National Science Foundation, U.S.A. (Corresponding author: Hanjun Kim)

Availability

The source code of DaCapo will be accessible to the public at `https://github.com/corelab-src/elasm`.

References

[1] Lattigo v4. Online: https://github.com/tuneinsight/lattigo, August 2022. EPFL-LDS, Tune Insight SA.

[2] Ahmad Al Badawi, Jack Bates, Flavio Bergamaschi, David Bruce Cousins, Saroja Erabelli, Nicholas Genise, Shai Halevi, Hamish Hunt, Andrey Kim, Yongwoo Lee, et al. Openfhe: Open-source fully homomorphic encryption library. In *Proceedings of the 10th Workshop on Encrypted Computing & Applied Homomorphic Cryptography*, pages 53–63, 2022.

[3] Ahmad Al Badawi, Chao Jin, Jie Lin, Chan Fook Mun, Sim Jun Jie, Benjamin Hong Meng Tan, Xiao Nan, Khin Mi Mi Aung, and Vijay Ramaseshan Chandrasekhar. Towards the alexnet moment for homomorphic encryption: Hcnn, the first homomorphic cnn on encrypted data with gpus. *IEEE Transactions on Emerging Topics in Computing*, 9(3):1330–1343, 2020.

[4] David W. Archer, José Manuel Calderón Trilla, Jason Dagit, Alex Malozemoff, Yuriy Polyakov, Kurt Rohloff, and Gerard Ryan. RAMPARTS: A Programmer-Friendly System for Building Homomorphic Encryption Applications. In *Proceedings of the 7th ACM Workshop on Encrypted Computing & Applied Homomorphic Cryptography*, WAHC'19, pages 57–68. ACM, 2019.

[5] Fabian Boemer, Anamaria Costache, Rosario Cammarota, and Casimir Wierzynski. ngraph-he2: A high-throughput framework for neural network inference on encrypted data. In *Proceedings of the 7th ACM Workshop on Encrypted Computing & Applied Homomorphic Cryptography*, pages 45–56, 2019.

[6] Fabian Boemer, Yixing Lao, Rosario Cammarota, and Casimir Wierzynski. ngraph-he: a graph compiler for deep learning on homomorphically encrypted data. In *Proceedings of the 16th ACM International Conference on Computing Frontiers*, pages 3–13, 2019.

[7] Zvika Brakerski, Craig Gentry, and Shai Halevi. Packed Ciphertexts in LWE-Based Homomorphic Encryption. In Kaoru Kurosawa and Goichiro Hanaoka, editors, *Public-Key Cryptography - PKC 2013*. Springer, 2013.

[8] Zvika Brakerski, Craig Gentry, and Vinod Vaikuntanathan. (leveled) fully homomorphic encryption without bootstrapping. In *Proceedings of the 3rd Innovations in Theoretical Computer Science Conference*, ITCS '12, pages 309–325, New York, NY, USA, 2012. Association for Computing Machinery.

[9] Sergiu Carpov, Paul Dubrulle, and Renaud Sirdey. Armadillo: a compilation chain for privacy preserving applications. In *Proceedings of the 3rd International Workshop on Security in Cloud Computing*, pages 13–19, 2015.

[10] Jung Hee Cheon, Kyoohyung Han, Andrey Kim, Miran Kim, and Yongsoo Song. Bootstrapping for approximate homomorphic encryption. In *Advances in Cryptology–EUROCRYPT 2018: 37th Annual International Conference on the Theory and Applications of Cryptographic Techniques, Tel Aviv, Israel, April 29-May 3, 2018 Proceedings, Part I 37*, pages 360–384. Springer, 2018.

[11] Jung Hee Cheon, Kyoohyung Han, Andrey Kim, Miran Kim, and Yongsoo Song. A full rns variant of approximate homomorphic encryption. In Carlos Cid and Michael J. Jacobson Jr., editors, *Selected Areas in Cryptography – SAC 2018*, pages 347–368, Cham, 2018. Springer International Publishing.

[12] Jung Hee Cheon, Andrey Kim, Miran Kim, and Yongsoo Song. Homomorphic encryption for arithmetic of approximate numbers. In *Advances in Cryptology–ASIACRYPT 2017: 23rd International Conference on the Theory and Applications of Cryptology and Information Security, Hong Kong, China, December 3-7, 2017, Proceedings, Part I 23*, pages 409–437. Springer, 2017.

[13] Eduardo Chielle, Oleg Mazonka, Homer Gamil, Nektarios Georgios Tsoutsos, and Michail Maniatakos. E3: A framework for compiling c++ programs with encrypted operands. Cryptology ePrint Archive, Report 2018/1013, 2018. https://ia.cr/2018/1013.

[14] Ilaria Chillotti, Nicolas Gama, Mariya Georgieva, and Malika Izabachène. Tfhe: Fast fully homomorphic encryption over the torus. *Journal of Cryptology*, 33(1):34–91, 2020. https://doi.org/10.1007/s00145-019-09319-x.

[15] Cingulata. https://github.com/CEA-LIST/Cingulata, 2020.

[16] Eric Crockett, Chris Peikert, and Chad Sharp. Alchemy: A language and compiler for homomorphic encryption made easy. In *Proceedings of the 2018 ACM SIGSAC Conference on Computer and Communications Security*, pages 1020–1037, 2018.

[17] DARPA. Darpa selects researchers to accelerate use of fully homomorphic encryption. https://www.darpa.mil/news-events/2021-03-08, March 2021.

[18] Roshan Dathathri, Blagovesta Kostova, Olli Saarikivi, Wei Dai, Kim Laine, and Madan Musuvathi. EVA: An encrypted vector arithmetic language and compiler for efficient homomorphic computation. In *Proceedings of the 41st ACM SIGPLAN Conference on Programming Language Design and Implementation*. ACM, 2020.

[19] Roshan Dathathri, Olli Saarikivi, Hao Chen, Kim Laine, Kristin Lauter, Saeed Maleki, Madanlal Musuvathi, and Todd Mytkowicz. CHET: An Optimizing Compiler for Fully-homomorphic Neural-network Inferencing. In *Proceedings of the 40th ACM SIGPLAN Conference on Programming Language Design and Implementation*. ACM, 2019.

[20] Junfeng Fan and Frederik Vercauteren. Somewhat practical fully homomorphic encryption. Cryptology ePrint Archive, Report 2012/144, 2012. https://eprint.iacr.org/2012/144.

[21] FullRNS-HEAAN. https://github.com/KyoohyungHan/FullRNS-HEAAN, 2018.

[22] Craig Gentry. Fully homomorphic encryption using ideal lattices. In *Proceedings of the forty-first annual ACM symposium on Theory of computing*, pages 169–178, 2009.

[23] Shai Halevi and Victor Shoup. Algorithms in helib. In Juan A. Garay and Rosario Gennaro, editors, *Advances in Cryptology – CRYPTO 2014*, pages 554–571, Berlin, Heidelberg, 2014. Springer Berlin Heidelberg.

[24] Kaiming He, Xiangyu Zhang, Shaoqing Ren, and Jian Sun. Deep residual learning for image recognition. In *Proceedings of the IEEE conference on computer vision and pattern recognition*, pages 770–778, 2016.

[25] HEaaN HE Library. https://heaan.it, 2022.

[26] HElib Open-Source HE Library. https://github.com/homenc/HElib, 2020.

[27] Andrew G Howard, Menglong Zhu, Bo Chen, Dmitry Kalenichenko, Weijun Wang, Tobias Weyand, Marco Andreetto, and Hartwig Adam. Mobilenets: Efficient convolutional neural networks for mobile vision applications. *arXiv preprint arXiv:1704.04861*, 2017.

[28] Zhicong Huang, Wen-jie Lu, Cheng Hong, and Jiansheng Ding. Cheetah: Lean and fast secure {Two-Party} deep neural network inference. In *31st USENIX Security Symposium (USENIX Security 22)*, pages 809–826, 2022.

[29] Forrest N Iandola, Song Han, Matthew W Moskewicz, Khalid Ashraf, William J Dally, and Kurt Keutzer. Squeezenet: Alexnet-level accuracy with 50x fewer parameters and< 0.5 mb model size. *arXiv preprint arXiv:1602.07360*, 2016.

[30] Chiraag Juvekar, Vinod Vaikuntanathan, and Anantha Chandrakasan. {GAZELLE}: A low latency framework for secure neural network inference. In *27th {USENIX} Security Symposium ({USENIX} Security 18)*, pages 1651–1669, 2018.

[31] Alex Krizhevsky, Ilya Sutskever, and Geoffrey E Hinton. Imagenet classification with deep convolutional neural networks. *Communications of the ACM*, 60(6):84–90, 2017.

[32] Nishant Kumar, Mayank Rathee, Nishanth Chandran, Divya Gupta, Aseem Rastogi, and Rahul Sharma. Cryptflow: Secure tensorflow inference. In *2020 IEEE Symposium on Security and Privacy (SP)*, pages 336–353. IEEE, 2020.

[33] Chris Lattner, Mehdi Amini, Uday Bondhugula, Albert Cohen, Andy Davis, Jacques Pienaar, River Riddle, Tatiana Shpeisman, Nicolas Vasilache, and Oleksandr Zinenko. Mlir: Scaling compiler infrastructure for domain specific computation. In *2021 IEEE/ACM International Symposium on Code Generation and Optimization (CGO)*, pages 2–14. IEEE, 2021.

[34] Yann LeCun, Léon Bottou, Yoshua Bengio, and Patrick Haffner. Gradient-based learning applied to document recognition. *Proceedings of the IEEE*, 86(11):2278–2324, 1998.

[35] DongKwon Lee, Woosuk Lee, Hakjoo Oh, and Kwangkeun Yi. Optimizing homomorphic evaluation circuits by program synthesis and term rewriting. In *Proceedings of the 41st ACM SIGPLAN Conference on Programming Language Design and Implementation*, PLDI 2020, pages 503–518, New York, NY, USA, 2020. Association for Computing Machinery.

[36] Eunsang Lee, Joon-Woo Lee, Junghyun Lee, Young-Sik Kim, Yongjune Kim, Jong-Seon No, and Woosuk Choi. Low-complexity deep convolutional neural networks on fully homomorphic encryption using multiplexed parallel convolutions. In *International Conference on Machine Learning*, pages 12403–12422. PMLR, 2022.

[37] Eunsang Lee, Joon-Woo Lee, Jong-Seon No, and Young-Sik Kim. Minimax approximation of sign function by composite polynomial for homomorphic comparison. *IEEE Transactions on Dependable and Secure Computing*, 19(6):3711–3727, 2021.

[38] Joon-Woo Lee, HyungChul Kang, Yongwoo Lee, Woosuk Choi, Jieun Eom, Maxim Deryabin, Eunsang Lee, Junghyun Lee, Donghoon Yoo, Young-Sik Kim, et al. Privacy-preserving machine learning with fully homomorphic encryption for deep neural network. *IEEE Access*, 10:30039–30054, 2022.

[39] Yongwoo Lee, Seonyoung Cheon, Dongkwan Kim, Dongyoon Lee, and Hanjun Kim. ELASM: Error-latency-aware scale management for fully homomorphic encryption. In *32st USENIX Security Symposium (USENIX Security 23)*, Anaheim, CA, August 2023. USENIX Association.

[40] Yongwoo Lee, Seonyoung Cheon, Dongkwan Kim, Dongyoon Lee, and Hanjun Kim. Performance-aware scale analysis with reserve for homomorphic encryption. In *Proceedings of the 28th ACM International Conference on Architectural Support for Programming Languages and Operating Systems*, ASPLOS 2024, La Jolla, CA, USA, 2024. ACM.

[41] Yongwoo Lee, Seonyeong Heo, Seonyoung Cheon, Shinnung Jeong, Changsu Kim, Eunkyung Kim, Dongyoon Lee, and Hanjun Kim. HECATE: Performance-Aware Scale Optimization for Homomoprhic Encryption Compiler. In *2022 IEEE/ACM International Symposium on Code Generation and Optimization (CGO)*, 2022.

[42] Vadim Lyubashevsky, Chris Peikert, and Oded Regev. On ideal lattices and learning with errors over rings. In Henri Gilbert, editor, *Advances in Cryptology – EUROCRYPT 2010*, Berlin, Heidelberg, 2010. Springer.

[43] Raghav Malik, Kabir Sheth, and Milind Kulkarni. Coyote: A compiler for vectorizing encrypted arithmetic circuits. In *Proceedings of the 28th ACM International Conference on Architectural Support for Programming Languages and Operating Systems, Volume 3*, pages 118–133, 2023.

[44] Pratyush Mishra, Ryan Lehmkuhl, Akshayaram Srinivasan, Wenting Zheng, and Raluca Ada Popa. Delphi: a cryptographic inference system for neural networks. In *Proceedings of the 2020 Workshop on Privacy-Preserving Machine Learning in Practice*, pages 27–30, 2020.

[45] Marie Paindavoine and Bastien Vialla. Minimizing the number of bootstrappings in fully homomorphic encryption. In *Selected Areas in Cryptography–SAC 2015: 22nd International Conference, Sackville, NB, Canada, August 12–14, 2015, Revised Selected Papers 22*, pages 25–43. Springer, 2016.

[46] PALISADE Lattice Cryptography Library. https://palisade-crypto.org/, October 2020.

[47] Deevashwer Rathee, Mayank Rathee, Nishant Kumar, Nishanth Chandran, Divya Gupta, Aseem Rastogi, and Rahul Sharma. Cryptflow2: Practical 2-party secure inference. In *Proceedings of the 2020 ACM SIGSAC Conference on Computer and Communications Security*, pages 325–342, 2020.

[48] Microsoft SEAL (release 4.1). https://github.com/Microsoft/SEAL, January 2023. Microsoft Research, Redmond, WA.

[49] Karen Simonyan and Andrew Zisserman. Very deep convolutional networks for large-scale image recognition. *arXiv preprint arXiv:1409.1556*, 2014.

[50] Alexander Viand, Patrick Jattke, Miro Haller, and Anwar Hithnawi. Heco: Automatic code optimizations for efficient fully homomorphic encryption. *arXiv preprint arXiv:2202.01649*, 2022.

[51] Alexander Viand and Hossein Shafagh. Marble: Making fully homomorphic encryption accessible to all. In *Proceedings of the 6th Workshop on Encrypted Computing amp; Applied Homomorphic Cryptography*, WAHC '18. Association for Computing Machinery, 2018.

[52] Alexander Wood, Kayvan Najarian, and Delaram Kahrobaei. Homomorphic encryption for machine learning in medicine and bioinformatics. *ACM Computing Surveys (CSUR)*, 53(4):1–35, 2020.

[53] Zama. Concrete: TFHE Compiler that converts python programs into FHE equivalent, 2022. https://github.com/zama-ai/concrete.

[54] Zama. TFHE-rs: A Pure Rust Implementation of the TFHE Scheme for Boolean and Integer Arithmetics Over Encrypted Data, 2022. https://github.com/zama-ai/tfhe-rs.

Appendix A Existing RNS-CKKS Compilers

Existing RNS-CKKS compilers propose automatic scale management schemes that insert scale management operations like `rescale` and `modswitch` to the input program that does not include scale management operations with optimizing performance and error.

EVA [18] proposes the first scale management algorithm that attempts to minimize the accumulated scale. A smaller accumulated scale is preferred as it allows the compiler to use smaller encryption parameters coefficient modulus Q and polynomial modulus N at the same security level, which in turn is expected to result in better performance. To this end, EVA regards the minimum scale of input ciphertexts to a program as the minimum scale requirement, called *waterline* S_w, of all ciphertexts. Then it inserts a `rescale` operation if the scale after rescaling is higher than the waterline: *i.e.,* $m/S_f \geq S_w$. Besides, EVA uses `upscale` and `modswitch` to meet the same level and scale requirements of arithmetic operations as needed.

Hecate [41] introduces a new scale management operation, called *downscale*, which combines `upscale` and `rescale` operations and supports decreasing the scale of a ciphertext by an arbitrary amount. Note that `rescale` can only reduce the scale by the fixed rescale factor S_f. Hecate makes use of the downscale operation to proactively bring the scale of a ciphertext down to the waterline S_w, and shows that it can achieve a lower accumulated scale than EVA. Furthermore, Hecate shows that a lower accumulated scale does not always lead to better performance, and presents a greedy latency-aware scale management algorithm based on static cost estimation. Recall that scale management operations `modswitch` and `rescale` change the levels of ciphertexts, affecting the latencies of the following arithmetic and rotation operations (Table 2). Combined with `downscale` and a greedy search algorithm, Hecate demonstrates a better performance (lower latency) than EVA.

ELASM [39] improves Hecate by reflecting the noise of RNS-CKKS operations. Because the RNS-CKKS operations add operation-specific and scale-independent noise to the result, the scale of the result affects the error of the operation by dividing the noise by the scale. To incorporate error awareness into the scale management scheme, ELASM proposes a noise-aware waterline that controls the waterline of each operation in a fine-grain manner reflecting the operation noise. To control the error level, ELASM controls the waterline based on the user-level compilation parameter called Scale-to-Noise-Ratio (SNR). Furthermore, ELASM proposes an efficient error estimator and error-aware exploration-based optimizer called Error-Latency-Aware Scale Management (ELASM) based on the error estimation. Combined with a noise aware waterline and an efficient error estimation scheme, ELASM achieves 4.2-bits better error and 16.7% better performance compared to Hecate.

Table 6: Function Parameters of AlexNet. Based on the multiplexed parallel packing method presented in [36], we implemented the convolution and pooling layers, using the same parameter notation.

Layer	n_i	n_o	f_h	f_w	s	h_i	h_o	w_i	w_o	c_i	c_o	k_i	k_o	t_i	t_o	p_i	p_o	q
ConvBN1	1	2	3	3	1	32	32	32	32	3	96	1	1	3	96	16	1	6
AvgPool1	2	1	3	3	2	32	16	32	16	96	96	1	2	96	24	1	2	96
ConvBN2	1	1	5	5	1	16	16	16	16	96	256	2	2	24	64	2	1	128
AvgPool2	1	1	3	3	2	16	8	16	8	256	256	2	4	64	16	1	4	256
ConvBN3	1	1	3	3	1	8	8	8	8	256	384	4	4	16	24	4	2	96
ConvBN4	1	1	3	3	1	8	8	8	8	384	384	4	4	24	24	2	2	192
ConvBN5	1	1	3	3	1	8	8	8	8	384	256	4	4	24	16	2	4	128
AvgPool3	1	1	3	3	2	8	4	8	4	256	256	4	8	16	4	4	16	64

Appendix B Parameters Used in Evaluation

Table 6 shows the function parameters that are used in each component of the AlexNet structure. ConvBN refers to a function that combines convolution and batch normalization, and AvgPool represents average pooling. The implementation of convolution and pooling layers is based on the paper from [36]. n_i and n_o denote the numbers of input and output ciphertexts. The tuples $\{w_i, h_i, c_i\}$, $\{w_o, h_o, c_o\}$ represent input and output tensors. A kernel with a size $f_w \times f_h$ strides by s. The remaining parameters such as k_i,k_o,t_i,t_o,p_i,p_o, and q are related to the multiplexed parallel convolution method presented in [36] Finally, the fully connected layer is implemented using the diagonal method in [23].